

Dalorex: A Data-Local Program Execution and Architecture for Memory-bound Applications

Marcelo Orenes-Vera, Esin Tureci, David Wentzlaff and Margaret Martonosi

Department of Computer Science, Princeton University

Princeton, New Jersey, USA

Email: {movera, esin.tureci, wentzlaf, mrm}@princeton.edu

Abstract—Applications with low data reuse and frequent irregular memory accesses, such as graph or sparse linear algebra workloads, fail to scale well due to memory bottlenecks and poor core utilization. While prior work that utilizes prefetching, decoupling, or pipelining can mitigate memory latency and improve core utilization, memory bandwidth bottlenecks persist due to limited off-chip bandwidth. Approaches using in-memory processing (PIM) with Hybrid Memory Cube (HMC) surpass DRAM bandwidth limitations but fail to achieve high core utilization due to poor task scheduling and synchronization overheads. Moreover, the granularity of the memory available to each processing core with HMC limits the level of parallelism.

This work proposes Dalorex, a hardware-software co-design that achieves high parallelism and energy efficiency, demonstrating strong scaling with >16,000 cores when processing graph and sparse linear algebra workloads. Over the prior work in PIM, using both 256 cores, Dalorex improves performance and energy consumption by two orders of magnitude through (1) a tile-based distributed-memory architecture where each processing tile holds an equal amount of data, and all memory operations are local; (2) a task-based parallel programming model where tasks are executed by the processing unit that is co-located with the target data; (3) a network design optimized for irregular traffic, where all communication is one-way, and messages do not contain routing metadata; (4) a novel traffic-aware task scheduling hardware that maintains high core utilization; and (5) a data placement strategy improving work balance.

This work proposes architectural and software innovations to provide—to our knowledge—the fastest design for running graph algorithms, while still being programmable for other domains.

I. INTRODUCTION

System designs are increasingly exploiting heterogeneous, accelerator-rich designs to scale performance due to the slowing of Moore’s Law [39] and the end of Dennard Scaling [21], [51]. While compute-bound workloads thrive in an accelerator-rich environment, memory-bound workloads such as graph algorithms and sparse algebra present the following **challenges**: (1) a low compute-per-data ratio, where a lot of the data accessed is not reused; (2) frequent fine-grained irregular memory accesses that make memory hierarchies inefficient; (3) atomic accesses, synchronization, and an inherent load imbalance result in poor utilization of computing resources.

Recent work proposed using accelerators that pipeline the different stages of graph processing in hardware [1], [14], [19], [42], [46], [50]. Other works have used general-purpose cores with decoupling and prefetching, to mitigate memory latency issues [18], [37], [41], [44], [55], and coalescing, to reduce the serialization caused by atomic updates [40]. These

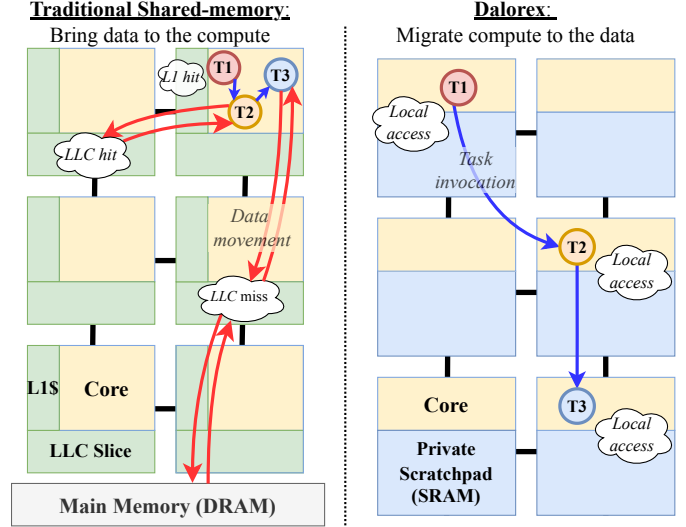


Fig. 1. Program execution of three sequential graph-processing steps in a cache hierarchy (left), and Dalorex (right). Instead of moving data with little reuse, Dalorex invokes tasks where the data is local—reducing movement.

solutions, however, fail to avoid costly data movements and are eventually bottlenecked by memory bandwidth. The proposals in the area of Processing-in-memory (PIM) enjoy a higher memory bandwidth by processing data near DRAM [2], [67], [72]. However, their memory technology choice constrains the **storage-per-core** ratio, limiting the level of parallelism—as we demonstrate later in this paper. In addition, their parallelization schemes suffer from load imbalance and synchronization overheads that undermine core utilization, as it also happens in other approaches described in Section II.

Opportunities: We started our work by examining what features are necessary to execute graph workloads in a scalable manner. We observed that in order to maintain high processor utilization and maximize throughput (edges processed per second), *the solution should*: (1) minimize data movement, which is the primary source of bottleneck and the most significant energy cost; (2) avoid global synchronization from barriers and read-modify-write atomic operations; (3) avoid frontier redundancy and data staleness to minimize the number of edges explored.

Our Approach: We present Dalorex, a hardware-software co-design that overcomes these challenges through a novel *programming model* that enables further parallelism by split-

ting the code into tasks at each pointer indirection. This removes the round trip time when accessing memory thanks to a tile-based *architecture design* where *all* memory accesses are local to the tile where the task is executed. In addition to the existing inter-loop interleavings (loop iterations may execute in any order and tile), the task splitting process provides more parallelism through intra-loop spatial interleavings (parts of the code within an iteration may execute in different tiles). We designed a specialized hardware task scheduling unit that orchestrates where tasks execute and in which order. Thanks to this unit, the communication between tiles is non-blocking and non-interrupting. Furthermore, we distribute the dataset equally across tiles to achieve uniform traffic on-chip, despite the irregular communication patterns of sparse workloads. As a result of this data partitioning, each tile owns a set of nodes (there are no copies of data), and all operations are intrinsically atomic. This also makes it very efficient for Dalorex to have a decentralized frontier and remove the global barrier between epochs of graph algorithms.

Dalorex is composed of a 2D-array of homogeneous tiles, each containing a thin in-order core (without caches) called the Processing Unit (PU), a task scheduling unit (TSU) that orchestrates the activities of the PU, an SRAM scratchpad, and a router connected to the network-on-chip (NoC). Dalorex does not have shared or virtual memory. Instructions are executed in the tile where the data is local. We study several NoC options for communication of tasks between tiles (Section III-F).

Fig. 1 illustrates how the distributed memory architecture of Dalorex (right panel) minimizes data movement over a hierarchical shared-memory architecture (left panel).

Memory hierarchies greatly benefit from data reuse. However, in the case of applications using sparse data, reuse distance is highly irregular, causing cache thrashing and resulting in more than 50% of all memory accesses to miss in the cache levels and going to main memory [37]. Shared memory architectures also carry the overhead of cache coherence, virtual memory, and atomic operations.

In contrast, with Dalorex (right panel of Fig. 1), each piece of data is only accessed by one PU. Instead of bringing data to the PUs, they send task-invoking messages to the tile containing the data to be processed next. Dalorex exploits the inherent pointer indirection of sparse data formats to route a task-invocation message. The tile’s PU executes the task corresponding to the message received. (A task might trigger another task at completion.)

To support this task communication scheme, our programming model assumes that the code is split at each indirect access to data arrays. Fig. 2 shows an example of how a graph algorithm is split into tasks. Section II uses this example to explain why its memory access pattern is challenging.

The technical contributions of this paper are:

- A data-local execution model where each processing tile holds an equal amount of data—operating on local data makes all updates atomic and minimizes data movement.
- A programming model that unleashes parallelism and improves work balance by splitting the code into tasks

```

1 while not frontier.isEmpty()
2   parallel for (v : frontier)
3     node_dist = dist[v]
4     startInd, endInd = ptr[v], ptr[v+1]
5     for i in range(startInd, endInd):
6       neighbor = edges[i]
7       new_dist = node_dist + edge_val[i]
8       curr_dist = dist[neighbor]
9       if (new_dist < curr_dist):
10        dist[neighbor] = new_dist
11        new_frontier.push(neighbor)
12 frontier = new_frontier
13 new_frontier = []

```

TASK 1
TASK 2
TASK 3

Fig. 2. Code of the Single Source Shortest Path (SSSP) algorithm, and how it is split into Dalorex tasks based on indirect memory accesses.

based on data location while preserving program order.

- A headerless communication scheme where task messages are routed by the index of the array they access.
- A hardware unit (TSU) that removes task-invocation overheads and schedules tasks to maximize core utilization and work efficiency by sensing the network traffic.

We evaluate Dalorex and demonstrate that:

- Our data distribution and parallelization does not require pre-processing to improve work balance across tiles. Dalorex remains agnostic to the dataset characteristics.
- Our data-local execution model improves *performance* by $6.2\times$ over the best ISA-programmable prior work [2]. On top of that, our task invocation mechanism improves by $4.7\times$, and our uniform data placement and traffic-aware scheduling, $4.4\times$ more. Finally, removing the barriers and upgrading the NoC provides an extra $1.8\times$, totalling a compound $221\times$ geomean improvement, across four key graph applications, using equal processor count (256).
- Regarding *energy consumption*, the compound improvements from having SRAM ($16\times$), data-local execution ($5.6\times$), and TSU ($4.7\times$) total $414\times$, in geomean.
- Dalorex achieves strong scaling with over 16,000 processing tiles, reaching the parallelization limit of the datasets.

II. BACKGROUND AND MOTIVATION

Dalorex is designed to accelerate applications that are memory-bound due to the irregular access pattern caused by pointer indirection. Graph algorithms are some of the most important workloads bottlenecked by irregular memory accesses. Although in this paper we focus on these, Dalorex is applicable to other domains such as sparse linear algebra. We demonstrate this by evaluating sparse matrix-vector multiplication.

A. Graph Algorithms and their Memory Access Patterns

Graphs are represented using huge adjacency matrices where rows/columns represent vertices and values represent weighted edges. Since the columns contain mostly zero values (most vertices have few connections), these matrices are stored in compact formats like Compressed-Sparse-Row (CSR) using four arrays. The indices of non-zero elements and their values are accessed via pointer indirection.

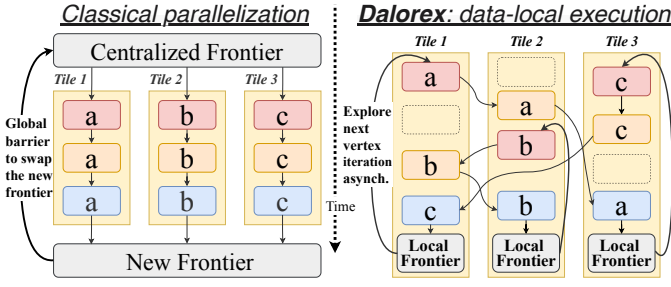


Fig. 3. Program order and synchronization for Bulk Synchronous Parallel (BSP), left, versus Dalorex model, in the right side. The yellow columns are the tasks executed in each tile (arrows indicate program order). Within them, the color indicates the task type, based on the code of Fig. 2, while the letters represent different vertex iterations.

Fig. 2 shows the code for Single Source Shortest Path (SSSP) and the corresponding Dalorex tasks. In a regular memory hierarchy, the accesses to neighbor vertex data in the innermost loop (line 8) result in many cache misses, and thus, in costly accesses to DRAM [37]. Moreover, the source vertex data (lines 3 and 4) and the neighbor index (line 6) are also accessed indirectly, and the utility of the cache depends on the number of neighbors and the workload distribution.

In Dalorex, the code is split at each level of pointer indirection, leading to a series of tasks. On the code of Fig. 2, TASK 1 accesses **dist** and **ptr** arrays (tuple of size $\#vertices$), TASK 2 accesses **edge** and **edge_value** arrays (tuple of size $\#edges$), and TASK 3 accesses again the **dist** array.

As Fig. 3 illustrates, Dalorex allows *spatial interleavings within vertex iterations* while preserving program order through the sequential invocation of the tasks. Like with classical parallelization, time-wise interleavings of different for-loop iterations are also allowed. Finally, instead of using a centralized frontier, Dalorex uses local frontiers, which removes the synchronization overheads of frontier insertions and global barriers. As a result, our novel programming model maximizes the parallelization of our data-distributed architecture.

B. Algorithmic variants

There are two modes of processing graph data: pulling data for a vertex from its neighbors or pushing data to its neighbors [7]. While pull-based algorithms tend to require higher memory communication, push-based algorithms often require atomic operations. When atomic operations can be avoided, push-based algorithms offer advantages through reduced communication overhead. A hybrid version, direction-optimized *BFS* [5], and its variants can offer faster convergence. However, they incur a storage overhead and need heuristics, as they may access either the source or the destination of an edge. Although pull-based algorithms can be executed on the Dalorex architecture, in this work we focus on push-based algorithms due to their communication and work efficiency.

In push-based parallel algorithms, neighbors of several vertices are updated concurrently. Since these vertices may

overlap neighbors, shared memory implementations require using atomic operations. This puts pressure on the coherence protocol to guarantee reading correct values for read-after-write operations, incurring additional memory latency.

C. Prior Work

In this section, we describe prior work that utilized pipelining and data-movement-reducing techniques, and we lay out what aspects of these designs fell short of achieving highly scalable parallelization.

1) *Hardware Techniques*: Recent works have used decoupling to overlap data fetch and computation by running ahead in the loop iterations to bring the data asynchronously [37], [41], [44], [55]. To accomplish this, they perform program slicing on each software thread, creating a software pipeline effect. Others have proposed accelerators to perform the graph search as a hardware pipeline [1], [14], [19], [46], [50]. Polygraph [14] generalized prior accelerator designs to perform any of their algorithmic variants and optimize work efficiency based on dataset characteristics. While effective for hiding latency, these approaches still suffer from excessive data movement and are ultimately limited by DRAM bandwidth.

To increase memory bandwidth and reduce data movement Tesseract [2] proposed in-memory graph processing by having groups of cores in the logic layer of a 3D integration, accessing a Hybrid Memory Cube (HMC) [24], [47] and utilizing remote function calls to be executed by cores located near the data.

However, the performance of PIM-based approaches is limited because: (1) Their vertex-based data distribution scheme causes significant load imbalance since the highly variable number of edges per vertex in graphs cause different amount of work per core; (2) Tesseract [2] uses interrupting remote procedure calls, which incur high cycle penalties, and the solution to avoid these interrupts proposed by GraphQ [72] employs many barriers to batch communication, causing high synchronization overheads; (3) HMC-based architectures are constrained in the number of cores per cube, which is tied to the number of vaults limiting the strong scaling to a data size of 512MB per core. In this paper, we explore the limits of graph parallelization and demonstrate that the energy-optimal storage size per tile is in the kilobytes range, far below the HMC range.

Finally, these prior hardware solutions utilize programming models with synchronous frontier parallelization through global barriers. This, as we see in the next section, can be detrimental to the overall performance of execution.

2) *Software Techniques*: Software solutions to accelerating graph applications include (1) optimizing data placement, work efficiency, and parallelization schemes based on target hardware [68]; (2) exploration of barrierless and asynchronous models [20]; and (3) vertex-centric execution schemes [36].

Designed for distributed systems, GiraphUC [20] puts forward a Barrierless-Asynchronous-Parallel model that reduces message staleness and removes global synchronization barriers. However, this approach is not optimized for data locality and therefore has high communication costs.

Pregel [36], on the other hand, parallelizes tasks such that each iteration is executed in a data-local and parallel manner but the data is distributed in a vertex-centric manner resulting in inherent load balancing problems in addition to communication overhead.

D. Manycore Architectures & Memory Bandwidth

Large-scale parallel processing can be done using many small processing elements. From Systolic arrays [25], [26], [32] and streaming architectures [23], [56], [57], to modern manycores [4], [15], [17], [65], challenges remain in the data supply on memory-bound applications.

Recently, some industry products have utilized large amounts of SRAM to achieve high on-chip bandwidth and thus higher performance [9], [29]. Aside from energy consumption, there are architectural advantages of using scratchpad memories that are tightly connected to cores: (1) There is no access contention as each core has dedicated access to its local memory, resulting in a higher per-core bandwidth; (2) SRAM has very low latency, removing the need for caches and prefetchers; (3) SRAM is more energy-efficient than DRAM, especially for fine-grain accesses, where DRAM has the overhead of opening and closing memory rows.

III. DALOREX: A HARDWARE-SOFTWARE CO-DESIGN

Dalorex minimizes data movement and maximizes resource utilization with: (1) a data distribution that allows for *only* local memory operations; (2) a programming model that allows for intra-loop spatial and inter-loop timewise interleavings; (3) a homogeneous tile-based architecture that optimizes irregular data-access patterns, where each tile includes a local memory, a router, and a processing unit. Program execution is orchestrated by the task scheduling unit.

A. Data distribution

As mentioned, graphs and sparse matrices are often stored in compact formats like CSR using four data arrays. In Dalorex, these arrays are divided equally across all tiles and stored in tiles' private memories, making each tile responsible for operations on its local data. For example, the `edge_values` array has as many elements as edges (E) in a graph. This array is split as in Listing 1 so that each of the T tiles allocated to run the program has `EDGES_PER_CHUNK` (E/T) adjacent elements, e.g., the first tile contains elements from 0 to `EDGES_PER_CHUNK-1`.

Ours is the first work that distributes an adjacency matrix in this manner; the usual approach is to do a 2D distribution of the matrix [8], where each computing element gets a rectangular subset of the matrix to compute. Although designed to minimize communication, 2D distribution presents some challenges: a subset of a sparse matrix is hyper-sparse (making row or column sparse formats storage-inefficient), and the resulting chunks do not have an equal number of non-zeros (different storage needs). Because Dalorex aims to have all memory on-chip equally distributed across tiles, we designed it to embrace inter-tile communication by making it part of the programming model.

B. Programming model

BSP parallelizations of graph algorithms parallelize either the outer loop (processing of vertices in the frontier) or the inner loop (processing of neighbors of the frontier vertices) since these iterations can be processed in any order. We posit that if the inner loop's iterations are performed in program order, the location of execution can be altered. In Dalorex, the sequential order of the instructions within an iteration is preserved by allowing each task only to be invoked by the previous one. Since only one tile has access to each data chunk (the owner), coherence is not an issue.

Adapting a graph kernel to Dalorex involves splitting the inner loop iteration into multiple tasks at the point of each pointer indirection. This results in 4 tasks for graph applications, with each task producing the pointer for the next task's data access. Each tile contains the code to perform any task.

From the program execution timeline perspective, after each task is performed at its data location, the task's output, which is the input for the next task, is sent to the tile where the data to be operated next is located, preserving sequential order of the program.

However, from the point of view of an individual tile, inputs for all tasks can arrive in any order into their corresponding queues in the tile and can be processed in any order. The execution order is managed by the TSU—described in Section III-E. This scheme effectively pipelines tasks without moving data, as all operations on data are local.

C. Program Flow and Synchronization

Dalorex programs do not have a *main*. Instead, tiles await the task parameters to arrive in the corresponding input queue, and PUs are invoked by TSU to process them. A task may invoke the next task by placing the task parameters into an output queue (OQ). An OQ can be either a task-input queue (IQ) if the next task operates over data residing in the same tile or a channel queue (CQ), which puts a message into the network.

Listing 1 contains the code of the Dalorex-adapted SSSP kernel. To start running the SSSP example, only the tile containing the root of the graph search receives a message to invoke `task1`. This task obtains the range array indices that contain the neighbors of `vertex_id`. If this range crosses the border of a chunk, a separate message is sent to each tile with the corresponding *begin* and *end* indices. Similarly, the range is split if the length is bigger than a constant `MAX_T2`, that is set to guarantee that `task2` can execute without exceeding the capacity of `C2Q`. However, `task1` does not have this guarantee and needs to check explicitly that `C1Q` does not overflow. If `C1Q` fills before sending all the messages for `vertex_id` range, a flag is set and `task1` ends early after updating the *begin* index. The next time `task1` is invoked it continues operating on the same `vertex_id` since it was not popped from `T1Q`. Note that `vertex_id` was explicitly loaded with `peek`, as opposed to `task2` and `task3`, where the task parameters are implicitly popped from their IQs by TSU (Section III-E).


```

## These constants are filled when the program is loaded
param TILEID
param NODES_PER_CHUNK
param EDGES_PER_CHUNK
## Local chunk of the dataset arrays
var dist[NODES_PER_CHUNK]
var ptr[NODES_PER_CHUNK]
var edge_idx[EDGES_PER_CHUNK]
var edge_values[EDGES_PER_CHUNK]

const FRONTIER_LEN = NODES_PER_CHUNK/32
## Bitmap frontier and memory-stored variables
var frontier[FRONTIER_LEN] = [0,...,0]
var blocks_in_frontier = 0
var t1_new_node = True
var neighbor_begin = 0;

##Configure network channels between tasks and their queues
C1Q = channel(q_len=128, target=T2, enc=EDGES_PER_CHUNK)
C2Q = channel(q_len=1024,target=T3, enc=NODES_PER_CHUNK)

## Declaring a task requires the length of its input queue
## and whether its parameters are loaded before invocation
task T1 [32] ():
    node_id = peek(T1Q.head)
    if (t1_new_node):
        neighbor_begin = ptr[node_id]
        neighbor_end = ptr[node_id+1]
        ## Split msg if range crosses chunk limits, or > MAX_T2
        partial_end = min(neighbor_end, TILEID*NODES_PER_CHUNK)
        partial_end = min(partial_end, neighbor_begin+MAX_T2)
        while (!C1Q.full && neighbor_begin < partial_end):
            C1Q = neighbor_begin ## global idx for tile address
            C1Q = (partial_end % NODES_PER_CHUNK) ## local idx
            C1Q = dist[node_id]
            neighbor_begin = partial_end
        ## We pop node_id if the whole range was pushed to C1Q
        t1_new_node = (neighbor_begin == partial_end)
        if (t1_new_node):
            pop(T1Q.head)

task T2 [128] (neighbor_begin, neighbor_end, node_dist):
    for i in range(neighbor_begin,neighbor_end):
        ##Writing to a channel queue sends data to the network
        C2Q = edge_idx[i]
        C2Q = edge_values[i] + node_dist

task T3 [2048] (new_dist, neigh_id):
    curr_dist = dist[neigh_id]
    if (new_dist < curr_dist):
        dist[neigh_id] = new_dist

    ## Insert vertex into Local Frontier
    blk_id = neigh_id >> 5;
    blk_bits = frontier[blk_id];
    frontier[blk_id] = mask_in_bit(blk_bits, neigh_id)
    if (blk_bits == 0): ## only count active blocks
        blocks_in_frontier++
        if (!T4Q.full) T4Q = blk_id

task T4 [1024] ():
    frontier_block = peek(T4Q)
    while(blocks_in_frontier > 0 && !T1Q.full):
        blk_bits = frontier[frontier_block]
        block_base = frontier_block << 5;
        while(blk_bits > 0 && !T1Q.full):
            idx = search_msb(blk_bits)
            blk_bits = mask_out_bit(blk_bits, idx)
            vertex = block_base + idx
            T1Q = vertex

        if (blk_bits == 0):
            pop(T4Q)
            blocks_in_frontier--
            if (T4Q.empty) frontier_block =
                (frontier_block + 1) % FRONTIER_LEN
            else frontier_block = peek(T4Q)

```

Listing 1. Pseudo-code of the SSSP algorithm adapted to use the Dalorex programming model.

Continuing from Listing 1, task2 calculates the new distances to all the neighbors of vertex_id from root using their edge values and sends this value to the owner of task3 data. Then, task3 checks whether the distance of neigh_id from the root dist is smaller vertex_id than the previously stored value. If so, neigh_id needs to be inserted in the frontier.

When placing the parameters of the next task into a channel queue, the first one is the index of the distributed array to access next, so the message is bound to the tile whose local chunk contains that index (see Section III-E detailed explanation). Sending tasks to other tiles is akin to non-blocking remote function calls employed by Tesseract [2]. However, unlike Tesseract, Dalorex task invocations are non-interrupting. In addition, Dalorex divides the whole program into tasks that are executed where the data is local, not just the atomic update of the dist array. Finally, Dalorex does not use a barrier after each graph-search epoch to scatter the new global frontier. Instead, each tile has a local frontier, thus allowing for continuous execution flow of tasks.

The local frontier is a bitmap to accumulate updates to the vertices that a tile is responsible for (the ones within its chunk of the vertex array). task4 is responsible for re-exploring the local frontier. To avoid iterating over every 32-vertex block in the frontier when task4 is invoked, task3 pushes the ID of a new block to be explored (blk_id) into the IQ of task4. The frontier only needs to be fully iterated when blocks_in_frontier increases but T4Q is full.

Termination: The program ends when all tiles are idle. This is determined by aggregating a hierarchical, staged, idle signal from all the tiles (co-located with the clock and reset signals). Similar to a loosely-coupled accelerator [12], [48], the host gets an interrupt when the global idle signal is set, to notify that the work is completed.

Synchronization: Although we strive to avoid synchronization between graph epochs (so that each epoch does not take as long as the slowest tile), Dalorex also supports global synchronization by reusing the chip idle signal. To have synchronization per epoch, task3 should not push new frontier vertices into the IQ of task4 and just add them to the bitmap frontier. When all vertices are processed, the host detects that the chip is idle, and it sends a message to all tiles to trigger task4 and explore the new epoch. We provide a performance characterization with and without epoch synchronization in Section V.

Host: The host is a commodity CPU, that arranges the load of the program binary and the dataset and from disk to the Dalorex chip. The program, composed of tasks and memory-mapped software configurations, is distributed as a broadcast and therefore identical for all the allocated tiles. The data is distributed such that every tile receives an equal-size chunk of each array.

Dalorex does not use virtual memory, although the host processor can still use virtual addressing within its memory. This avoids the overheads of address translation, which are exacerbated in graph applications due to irregular memory

accesses. Another advantage of having private, uncontested access to memory is not needing to deal with memory coherence or consistency issues.

D. Graph size vs Chip size

Dalorex uses a homogeneous 2D layout of tiles. Because the size of a tile’s local memory is determined at fabrication time, the aggregated chip storage scales linearly with the computing capacity (see Section V-B for optimal storage to compute ratio). We envision Dalorex to be deployed at the edge with a 16×16 , 512 MB, 151mm^2 chip, or at data-centers with a 256×256 , 128GB, wafer-scale integration.

Processing Larger Graphs: Building on previous work on distributed graph processing [28], [59], we propose using graph partitioning to split larger graphs into multiple parts, where each part is computed on a separate Dalorex chip. The aggregated storage on chip determines the maximum size of a graph partition. Smaller graphs can also be computed concurrently in rectangular subsets of tiles within a chip, uncontested, as they do not share hardware resources. The tiles that are not allocated to run programs are switched off.

Selecting the number of tiles a program runs on has a lower bound: it should run a subset of Dalorex that is large enough to fit the dataset into the aggregated memory capacity. It can also choose to use a larger number of tiles to parallelize even further. Section V shows that Dalorex scales close to linearly until the parallelization limits are hit when a tile handles less than a thousand vertices.

E. Dalorex Hardware

Fig. 4 shows the structure of a tile in the Dalorex architecture. The Processing Unit (PU) is a very power- and area-efficient unit that resembles a single-issue, in-order core, but without a memory management unit or L1 cache, as the data is accessed directly from the scratchpad memory. The tile area is dominated by the scratchpad SRAM, which contains the data arrays, the code, and the entries of the input/output queues. The queues are implemented as circular FIFOs using the scratchpad. Queues sizes are configured at runtime, based on the number of entries specified next to the task declaration (see Listing 1). A queue entry can be either 32 or 64 bits, depending on the chip’s target total memory size. (A 32-bit Dalorex can process graphs of up to 2^{32} edges.)

The **Task Scheduling Unit** (TSU) is the key hardware unit of Dalorex’s hardware-software co-design. It contains the task configurations and scheduling policy and handles the queues’ head and tail pointers. The TSU has a read-write port into the scratchpad for pushing data from the router buffers to the input queue. From the other side, the tail and head pointers are exposed to software through Queue Specific Registers (QSR). QSRs allow the PU to read or write from its queues with a register operation, avoiding instructions to calculate the address. A read from a QSR results in a load from the scratchpad using the corresponding queue’s head pointer provided by the TSU. This read also triggers the update of the head pointer in hardware at the *Task Queue Status* table.

The TSU is responsible for invoking tasks based on the status of the IQ and OQs. Tasks cannot block, so TSU invokes a task only if its OQ has more than sixteen free entries (this sets the minimum configurable queue size) and IQ is not empty. TSU needs to arbitrate when two or more tasks have non-empty IQs. The queues’ occupancy acts as sensor information for the TSU to decide which task to prioritize. A task can have three modes of priority based on the occupancy of its IQ and OQ: high priority if its IQ is nearly full, medium priority if its OQ is nearly empty, and low priority otherwise. When two or more tasks have high priority, the one with a larger IQ size takes precedence. The same applies to medium priority with OQs.

After testing several static priorities and round-robin schemes, we found that this occupancy-based priority worked best for two reasons: (1) The primary source of network contention is end-point back-pressure, so preventing IQs from being full eases contention; (2) Reaching high resource utilization relies on tiles giving each other work, so keeping OQs non-empty is important. These heuristics are micro-coded as event-condition-action rules and are set based on the reaction time that it takes to prioritize a task and prevent the IQ from getting full or the OQ empty. When all IQs are empty, TSU disables the clock of the PU, to save power.

During program execution, if a task outputs parameters for the next task to be executed on another tile, a **channel queue** outputs the data to the network, which delivers the data to the destination. A **network channel** always connects a channel queue with a task’s IQ. Messages can be composed of several flits, each being a parameter of the task to be called. The network communication is composed of flits traveling in different logical channels that share the same network-on-chip (NoC). A flit has the same size as a queue entry, which is the width of the PU’s ALU and the memory addresses. (For our experiments, we evaluated a 32-bit Dalorex.)

The **routers** have bi-directional ports to north, south, east, west, and towards the tile’s TSU. Routing is determined by the router based on the data in the first flit of a message, which we call the *head*. Since the head flit always contains a dataset-array index, and these arrays are statically distributed across the chip, this index is used to obtain the destination tile. The TSU’s channel table contains the sizes of the local chunks and the number of parameters (flits) of a specific message type. The head encoder uses that information to calculate the destination tile and the local index (modulo the chunk size). The encoder also uses the width of the Dalorex rectangle to obtain the X/Y coordinates. Depending on the width and height of the chip, the upper bits of the head flit encode the destination tile ($\log_2(\text{width}) + \log_2(\text{height})$). Routers compare incoming head flits with their local X/Y tile ID to determine where to route it next. If routed to the TSU, the head decoder removes the tile index bits from the head flit before it pushes it to the IQ.

This payload-based routing saves network traffic as it does not use metadata. The length of messages at each channel is known, and its flits are always routed back to back since

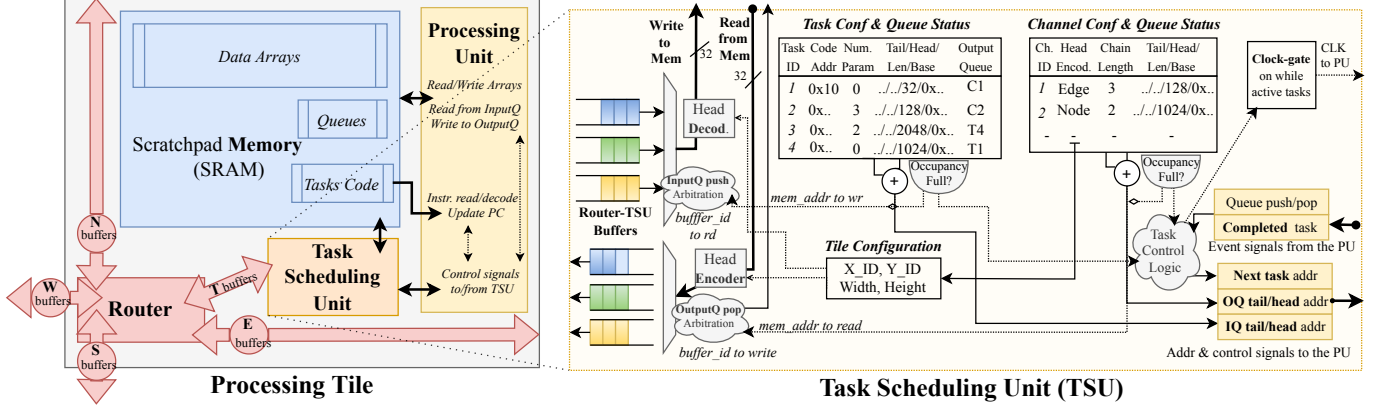


Fig. 4. Organization of a processing tile. TSU indicates the Processing Unit (PU) the next task to execute based on the occupancy of the task input queues (IQ). The router connects TSU with the network. TSU has a read-write port to the local memory to write incoming network data (push) to IQs and pop outgoing data from the channel queues (CQs).

a route (from input to output port) opens with the first flit and is closed after the corresponding number of flits has left the router. Interleaving flits from two messages going to the same output port on the same channel is not allowed. The router arbitrates by doing a round-robin between the messages from inputs ports that want to route to the same output port. However, the router can route to different outputs simultaneously.

Channels buffers: In addition to identifying the task type, communicating tasks in different channels prevents deadlocks. Although channels might contend to use the NoC, the routers contain buffers per channel so that a clogged channel does not block others. Each router has a pool of buffer slots per outbound direction shared between the channels. The size of this pool is a tapeout parameter, but the number of buffer slots per channel is software-configurable, as the sizes of the input/output queues.

F. Communication Network

Since Dalorex’s programming model uses task invocations that do not return a value, communication is one way only, resembling a software pipeline. Therefore, the communication latency between the sender and receiver tiles does not contribute to the execution time if the pipeline is full, i.e. task invocations are continuous. However, the throughput would suffer if bubbles are formed due to network contention.

Graphs are inherently irregular, and some vertices have much higher vertex-degree than others. These are often referred to as hot vertices. The channel buffers and queues mitigate the communication peaks caused by hot vertices and help keep the pipeline effect. Dalorex relies on random data distribution, so the number of hot vertices per tile is relatively uniform. Should the graph be sorted by vertex degree, we build the global CSR so that consecutive vertices fall into different tiles. This uniformity avoids excessive end-point contention at the TSU with messages from the router.

We observed that the network topology can be another source of contention. Dalorex uses a 2D-torus to avoid the contention towards the center we observed on a 2D-mesh. Our 2D-torus is a wormhole network with dimension-ordered routing. It also implements a local bubble routing to avoid the ring deadlock. This network can be fabricated with nearly equidistant wires by having consecutive logical tiles at a distance of two in the silicon. A 32-bit 2D-torus is 50% bigger than a 2D-mesh, but the torus provides twice the bisection bandwidth (BB) and 33% less number of hops [45].

Since we target the design of Dalorex to be scalable even with hundreds of tiles per dimension (tens of thousands of tiles), scalability of network utilization is part of the design goal. Scaling Dalorex up to the next power-of-two tiles per dimension results in four times the total tile count, but BB only doubles. While latency is greatly hidden by the pipeline effect, BB is critical for scalability since the vertex updates are irregular and result in communication to any tile. This disparity increases the contention with network sizes. To overcome that, we also explore ruche networks [27], [45].

Ruche networks are long physical wires that bypass routers. They increase the router radix and decrease the latency from source to destination. For example, in a network with a ruche factor of 2, a tile could route to their immediate neighbors or tiles at a distance of 2. A full ruche network of factor R increases the BB by a factor of $(R - 1) \times$ over the underlying network, so increasing sizes of R with larger network sizes can compensate for the previously observed BB decrease.

Dalorex does not assume or need ordered point-to-point communication between messages, so it can utilize ruche networks to skip tile hops if the destination is further than the ruche distance—in either X or Y direction. Section V provides a performance characterization of torus vs. mesh, with and without ruche networks.

G. Scalable Memory Bandwidth

Large scratchpads are more area-efficient with modern, smaller, FinFET transistor nodes [10], [16], [61]. This allows packing more SRAM on-chip than ever before. A real-world example is the Wafer-Scale integration of Cerebras, which enables 40GB of on-chip SRAM storage [35].

Having a dedicated scratchpad memory per tile enables immediate, uncontested access to memory. A memory port has a width equal to a network flit. The PU can make one memory read, and one write per cycle. This is leveraged by instructions writing to QSR from data arrays. The PU has another port to fetch instructions from the scratchpad. While the scratchpad has many banks, to save per-access energy, not all banks need to have all ports, e.g. the instruction port can exist only for a fraction of the local memory, setting a limit to the code size.

From a chip's perspective, since each PU has all the data it needs locally, the total memory bandwidth increase linearly with the number of tiles, unlike many modern hardware architectures. In the next section, we evaluate Dalorex in terms of program runtime and energy consumption when scaling the number of tiles.

IV. EVALUATION METHODOLOGY

This section first describes the widely-used workloads that we evaluated. Next, it explains our methodology to simulate and characterize Dalorex, along with the power and area model. Finally, it describes how we compare energy and performance with prior work.

A. Applications and Datasets

In addition to four graph algorithms, we evaluated one sparse linear algebra kernel to demonstrate the generality of our approach for memory-bound applications.

We adapted the following codes from the GAP benchmarks [6] and GraphIt [68], splitting the program into tasks at each indirect memory access: *Breadth-First Search (BFS)* determines the number of hops from a given seed vertex to all other vertices that can be reached from it; *Single-Source Shortest Path (SSSP)* finds the shortest path from the root to each reachable vertex; *PageRank* ranks websites based on the potential flow of users to each page [33]; *Weakly Connected Components (WCC)* finds all sets of vertices reachable from one another in at least one direction and labels them as belonging to the same component (we implement it using graph coloring [53]); *Sparse Matrix-Vector Multiplication (SPMV)* multiplies a sparse matrix with a dense vector.

Datasets: We perform the evaluation using real-world networks and synthetic datasets. We use several different sizes of synthetic RMAT graphs [34] of up to 67M vertices (V) and 1.3B edges (E), with up to 12GB of memory footprint, as well as real-world graphs: LiveJournal (V=5.3M, E=79M), Wikipedia (V=4.2M, E=101M) and Amazon (V=262K, E=1.2M).

B. Methodology

We decided to build a C++ simulator to evaluate Dalorex due to the novelty of the execution model and the simplicity of the architecture. This simulator is cycle-accurate for both message routing and task execution. While simulating the network, messages flow from tile to tile from source to destination, spending one cycle at each step. Our simulations are validated to provide correct program outputs over sequential x86 executions of the applications we evaluate [6].

Current architectures pay an enormous energy cost associated with accessing off-chip memory [43]. Thus, Dalorex has the potential to achieve great energy-efficiency improvements compared to prior work: reading data locally consumes nearly two orders of magnitude less energy than moving an equivalent block of data across 15mm of on-chip wire [22] and three orders of magnitude less energy than bringing the data from off-chip DDR3 [58].

Power and Area Model: Because of the latest technology improvements, SRAM can now achieve very high densities in FinFET, ranging from 29.2 Mb/mm² in 7nm [61] to 47.6 Mb/mm² in 5nm [10]. New technologies like FinFET or CMOS-ULVR show that leakage power can get as low as 1.7nW per cell [31], 5μW per 8KB (8192 bytes) macro [62], or 16.9μW for a 32KB macro at 7nm [61]. Although 5nm seems to be achievable today [16], we will be using the 7nm for our area and power models since this is a more mature transistor process, and we were able to find more reliable numbers for SRAM and logic. Reading a bank of data consumes 5.8pJ, and writing it 9.1pJ, with an access time of 0.82 ns [61]. Thus, we will use a 1GHz frequency for the system so that the memory access time fits within the cycle length.

In addition to using area-efficient SRAM technology, Dalorex uses processing units that resemble slim cores. We estimate the PU area considering the Celerity, Snitch, and Ariane cores [15], [64], [66]. To determine the dynamic and leakage power of the single-issue in-order core, we use the Ariane core [63] as a reference and transistor power scaling ratios to calculate the energy of those operations on a 7nm process [54], [60].

Regarding the NoC, we explore a 2D-Torus and a 2D-mesh, with and without ruche networks. These are modeled hop by hop between the routers, making the simulator precise for cycle count and energy. We use 8pJ as the energy to move a 32-bit flit one millimeter [38] and assume the energy of moving a flit at the router to be similar to an ALU operation. The NoC area is calculated based on Ou et al. [45].

These NoC options are explored in Fig. 7. For the rest of the results section, Dalorex uses a regular torus NoC with configurations up to 32×32 (1024 tiles) and a torus NoC with ruche channels for larger configurations.

C. Characterizing Dalorex

Dalorex can be fabricated with increasing sizes to scale on-chip memory and computing tiles. The aggregated memory capacity of a Dalorex chip can be obtained by multiplying the size of the local memory by the tile count. To determine the

local-memory size that achieves the highest energy efficiency, we evaluated increasing tile counts while keeping the same aggregated memory capacity (the dataset size). For this experiment, we ran BFS with four RMAT datasets of different sizes for every power-of-two configuration of Dalorex between 1×1 to 128×128 (16384 tiles), where the size of each tile’s memory decreases with the tile count.

Such an experiment also can reveal the limits of the parallelization: at which point the performance plateaus due to lack of work. Moreover, we show the performance scaling for the rest of the applications for the biggest RMAT dataset (over a billion edges).

In addition, we performed **sensitivity studies** to explore the PU and router utilization. We use heatmaps to show the percentage of the total runtime they are processing tasks or messages.

D. Comparison with the State-of-the-Art

Since graph algorithms are memory-bound, the most performant prior works utilize processing in memory (PIM). We compare the performance of Dalorex with Tesseract [2]. We also have simulated a more recent PIM-based approach GraphQ [72] which reported $3.3\times$ performance and $1.8\times$ energy improvements on average over Tesseract. However, despite communicating with the authors, we were unable to obtain the cycle and energy values from simulation outputs that matched their results. We do not include GraphQ in our discussion because the runtime and energy consumption we reproduced were $3.2\times$ and $4.6\times$ bigger (geomean), respectively, compared to these publications.

We simulate Tesseract using a Hybrid Memory Cube (HMC) configuration of 16 cores per cube (one per vault), aggregating a total of 256 cores among the 16 cubes. To match their core count, we use a 16×16 Dalorex configuration. To evaluate Tesseract work we follow their methodology by using the Zsim simulator [52] with the 3D-memory power model [49] (based on Micron’s disclosure for HMC). For the energy spent by the cores, we use the same power model as Dalorex—based on a 7nm transistor node. We compare runtime and energy performance for the duration of the graph processing time, not considering loading the dataset from disk to HMC or to the Dalorex chip.

We do not compare with commodity servers in the results section because Tesseract already demonstrated the advantage of PIM over systems where the main memory is off-chip. However, we collected the cycle count of our x86 server while validating the output of graph applications and observed that both the prior work and Dalorex perform better through their scalable memory bandwidth.

V. RESULTS

A. Improvements over the HMC-based prior work

In this section, we demonstrate the gains in performance and energy efficiency of Dalorex over Tesseract [2]. We **break down the contributions of the different optimizations of Dalorex** by: having 2MB private caches on Tesseract cores and

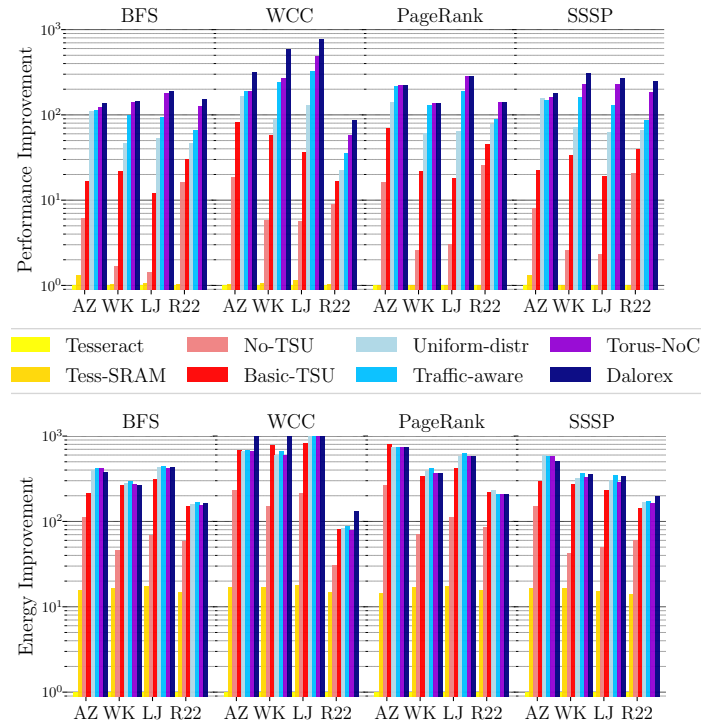


Fig. 5. Comparison of the performance and energy efficiency changes associated with several Dalorex features, normalized to Tesseract. X-axis studies four datasets. Y-axis is logarithmic, higher is better. Note that since PageRank necessitates per-epoch synchronization, the last datapoint (Dalorex) still uses a global barrier; thus, the bars do not change.

removing DRAM refresh energy to approximate the impact of using distributed SRAM on performance and energy (*Tess-SRAM*); removing TSU and using the program flow of Tesseract, where remote vertex updates are interrupting (*No-TSU*); having a basic TSU to invoke tasks with round robin scheduling (*Basic-TSU*); distributing the data arrays by lower order bits instead of higher order bits (*Uniform-distr*); having a scheduling policy that gives priority to tasks based on the occupancy of the input and output queues (*Traffic-aware*); using a 2D-Torus network instead of a 2D-Mesh (*Torus-NoC*); removing the global barrier after each epoch, reaching our full approach (*Dalorex*).

Section V-C further analyzes the impact of the NoC with another design that benefits larger Dalorex configurations.

Performance: Fig. 5 (above) shows that Dalorex substantially outperforms Tesseract across all datasets and applications. Our data-local execution model improves performance by $6.2\times$ (*No-TSU*). On top of that, TSU improves performance by $4.7\times$, and our uniform data placement and traffic-aware scheduling $4.4\times$ more. Finally, removing the barriers and upgrading the NoC provides an extra $1.8\times$, totaling a compound $221\times$ geomean improvement.

Synchronization in graph workloads causes each epoch to take as long as the slowest tile’s execution, increasing the total runtime. WCC benefits the most from barrierless processing due to having more epochs. Similarly, Wikipedia (WK) benefits most from removing the barrier as its graph structure leads to more epochs.

Energy: Fig. 5 (below) shows that the performance improvement of Dalorex over Tesseract, together with its power-efficient design, yields a very large improvement in energy consumption. The compound improvements from having SRAM (16 \times), data-local execution (5.6 \times) and TSU (4.7 \times) total a geomean on 414 \times . The breakdown shows that the energy spent on DRAM refreshing has the biggest impact on Tesseract (also concluded in their paper). Upgrading the NoC to a 2D-Torus increases energy usage by 7% geomean, besides being 40% faster. This is because the Torus network is more power hungry and has longer wires.

Area: The 16 \times 16 Dalorex with 4.2MB memory per tile uses much less chip area (305mm²), than the aggregated area of the 16 cubes of Tesseract (3616mm²). PIM-based approaches are limited by the constraints of HMC, having one core per DRAM vault of 512MB (8GB per cube). Most of this HMC storage is unused with the datasets that Tesseract evaluated (the empty bitlines of DRAM are switched off to save power). However, larger datasets would have a much bigger runtime in the HMC-based design, which cannot have more cores without increasing the number of cubes.

The prior work based on HMC is constrained by the number of cores that can be integrated into the logic die—often one per vault. HMC is also limited in scalability due to the large *power density*, which makes it more challenging to cool in 3D integrations [71]. Our power density is evenly distributed and stays below 300mW/mm² for all our experiments. This is much below the limits of air-cooled 2D chips ($\sim 1.5\text{W/mm}^2$ [69]).

Another limitation of the HMC-based approaches is that lower inter-cube *communication bandwidth* made their authors consider graph partitioning per cube, limiting the scalability of each partition. Our design is able to exploit the benefits of the programming model and allows tiles to send work to each other by having nearly zero overhead communication due to fast networks and lack of reception-interrupt.

To summarize, such large across-the-board improvements are achieved with a conjunction of optimizations at different levels of the software-hardware stack. Dalorex: (1) reduces data movement with its *fully* data-local program execution model, where only task parameters are moved, and there is no round-trip; (2) task invocations are natively supported through the TSU, so there are no interrupt overheads as in prior remote procedure calls; (3) does not require barrier synchronization between tiles for BFS, WCC, and SSSP; (4) coalesces vertex updates into its local frontier, minimizing redundancy; (5) utilizes SRAM to store the tile-distributed dataset, making data access immediate and energy-efficient for the challenging fine-grain irregular accesses. Also, SRAM is offered at finer sizes than DRAM, which allows using the energy-optimal memory-per-tile of a few megabytes that we found in the scaling experiment of the next section.

B. Dalorex Scales Beyond 10K Tiles

In the previous section, we evaluated using an equal number of processing units (256). Unlike Tesseract, Dalorex can efficiently parallelize further by distributing the dataset across

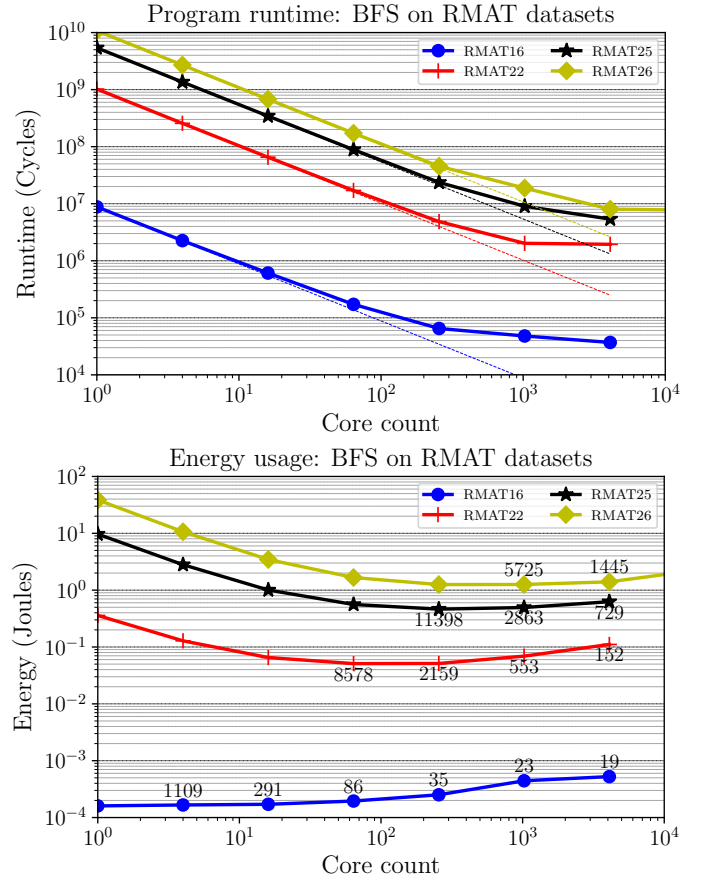


Fig. 6. Analysis of the runtime (cycles) and energy consumption (Joules) of BFS for four RMAT datasets and scaling core counts.

more tiles. To test for scalability of our architectural design, we evaluated the performance of Dalorex by running BFS for RMAT datasets of size 2¹⁶, 2²², 2²⁵ and 2²⁶ vertices (average ten edges per vertex).

Performance Scaling: The upper plot of Fig. 6 shows the runtime (in cycles) for each dataset on Dalorex with an increasing number of tiles by multiples of four. The most exciting result of this analysis is that Dalorex has a close to linear scaling until it hits the parallelization limit at the same time as the data chunk per core is $\sim 1,000$ vertices per tile regardless of dataset size. This indicates that what limits parallelization is *not* the communication or memory bandwidth (as is the case for all previous work) but tiles starving for work due to intrinsic parallelizability of graph processing.

Energy Scaling: To understand the optimal scratchpad size for energy consumption, we analyzed energy as the number of tiles increases and the necessary scratchpad size decreases. In this experiment, as parallelization increases, we fit the scratchpad size to the footprint of the dataset chunk, the program binary, and the queues.

Fig. 6 (below) shows total energy spent running BFS while increasing the number of tiles. Next to each datapoint is the memory used by each tile (in KB). As the tile count increases and the dataset chunk per tile becomes smaller, energy first reaches the optimal value and then increases. The consumption

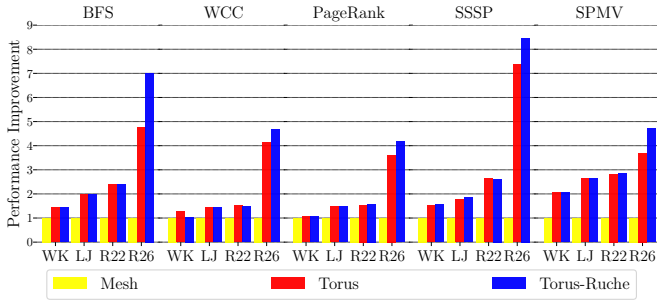


Fig. 7. Performance improvement of Torus and Torus-Tuche over Mesh. The X-axis shows the datasets used for each of the applications evaluated. RMAT-26 runs on 64×64 tiles, and the rest 16×16 .

initially decreases because, with very large scratchpad sizes, the workload of the application is not parallelized to the fullest extent. Therefore, the total execution time increases, making the leakage power of the SRAM storage more significant. As the dataset chunk per tile becomes smaller, at some point, the amount of work per tile is less than one task per tile at any given time, leading to work starvation by the cores, and the leakage power dominates.

The deflection point, i.e., minimal energy execution for each dataset, arrives when the amount of data per tile is $\sim 10,000$ vertices. As explained above, this impressive dataset-size invariant ratio is due to the scale-invariant parallelization capability of Dalorex. The smallest dataset, RMAT-16, reaches this point very early, having $\sim 1,000$ vertices per tile already with 64 tiles.

From Fig. 6 we can observe that the performance keeps scaling past the energy-optimal configuration. Unlike clusters, where performance degrades with small messages between computing nodes, Dalorex communication is at the granularity of a few words. Furthermore, scaling up to 16,384 tiles is not limited by bandwidth but by the parallelizability of the application running on each dataset. However, as we explore next, the NoC plays an essential role with large tile counts.

C. Characterizing the Network-on-Chip (NoC)

We will now analyze the three of the NoC types that we considered (see Section III-F): 2D-mesh, 2D-torus, and combining the torus with ruche channels. Fig. 7 compares their performance normalized to the mesh NoC. Using a 16×16 torus is nearly twice as fast as a mesh, on average, for the smaller datasets (Wikipedia, LiveJournal, and RMAT-22), which justifies the area cost of an additional 0.2% of the total chip area (using 2MB tiles).

We generated heatmaps for PUs and router utilization as a percentage of the total runtime to fully understand the reason for the superiority of torus with respect to mesh. Fig. 8 shows that the contention towards the center of the mesh (above) clogs the NoC and makes the PUs starve for tasks, whereas the torus (below) has a uniform router utilization, unleashing the full potential of the PUs. The torus becomes even more beneficial for the 64×64 , used to evaluate RMAT-26.

We also studied the impact of *ruche with torus* for several network sizes, and we found it to only improve 64×64

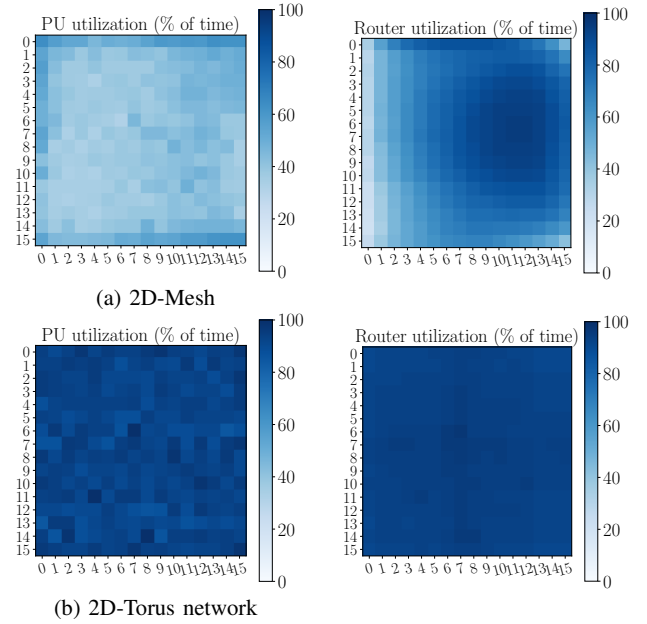


Fig. 8. Heatmaps of the utilization of PUs and routers while running SSSP on RMAT-22. The 16×16 tiles are connected by a mesh (above) or by a torus (below).

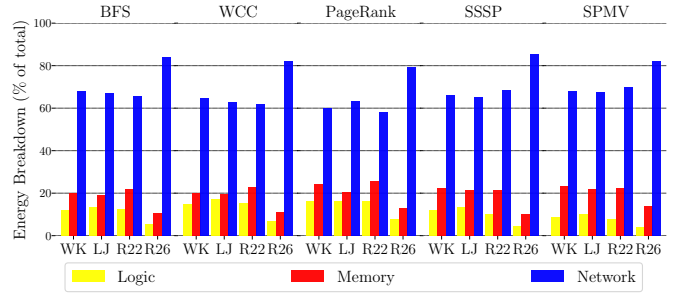


Fig. 9. Breakdown of the energy consumed by the computing logic, the SRAM cells and the network communication (including routing and wire energy). The Y-axis is the percentage of total energy spent running the program. The X-axis shows the datasets used for each of the applications evaluated. RMAT-26 runs on 64×64 tiles, while the rest on 16×16 tiles.

configurations and bigger datasets. Although a ruche-torus NoC costs more than twice the area of a regular torus (extra cost of 1.2% area) and higher power, the performance gains at large chip configurations justify its use. Although not shown here, we have found ruche combined with mesh not to be as effective as torus alone, despite its larger area cost.

Fig. 9 breaks down the energy consumed by Dalorex for our selected network: torus for the 16×16 configuration (WK, LJ, RMAT-22), and torus-ruche for 64×64 (RMAT-26). In Dalorex, the network consumes the most energy: the larger the network, the longer the average distance traveled to update a vertex, therefore a greater share of the total energy consumption. This is expected because, in addition to using SRAM, which lowers the contribution of memory storage, Dalorex has very simple processing units (PU) that only access local data. PUs are also not actively waiting for messages to arrive but are powered off by TSU when idle.

Throughput: Fig. 10 shows the number of edges and total

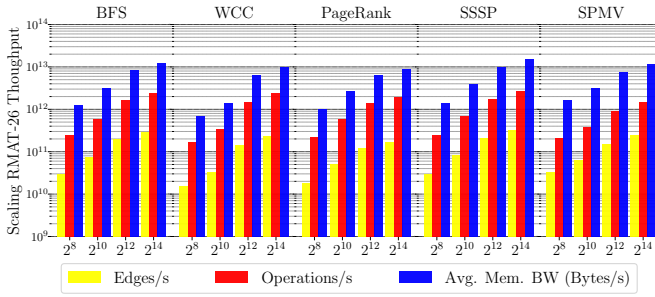


Fig. 10. Throughput in terms of software operations and edges explored per second, and the average on-chip memory bandwidth (BW) that was used to achieve that. The X-axis is the number of tiles of the Dalorex configuration used when analyzing strong scaling RMAT-26, across several applications. The Y-axis is logarithmic.

of operations processed per second as a measure of the throughput, and the aggregated BW used by tiles with their local memory as a measure of the average memory bandwidth (BW) used by Dalorex. We study this with doubling counts on X- and Y-dimension and for all of our benchmarks running our biggest RMAT dataset.

We observe that throughput, and thus the average BW utilized, grow until the largest configuration we simulated: 128×128 (2^{14} tiles). This last configuration reaches 2 tera-operations/s, using over 10 terabytes/s of memory. The throughput that Dalorex can achieve for graph applications is beyond the reach of the 3D-memory integration that Tesseract proposed.

As a testament to how large manycore designs need scalable BW to speed up these applications, Dalorex design provides a memory BW that does not saturate. This is possible by having all the memory storage distributed across tiles and linearly increasing the number of memory ports with the tile count. The fact that the memory BW does not saturate allows the PUs to keep processing vertices and edges, and the very high rates are shown in Fig. 10.

Since the communication queues are mapped into the local memory, receiving or sending task parameters also access memory. Also, note that this is the average BW of the whole program and not the maximum utilized at a given time. The peak memory BW available only increases with the number of tiles, and it is 131TB/s on a 128×128 Dalorex.

VI. FURTHER RELATED WORK & DISCUSSION

Due to storage limitations, graph networks that have trillions of edges inevitably need to be partitioned and processed by multiple systems. However, within each system (where most of the work will occur), distributed graph processing frameworks [3], [36], [59], [70] are bottlenecked by the memory hierarchies in current computer architectures.

Dalorex, and other HMC-based approaches for graph processing [2], [67], [72] behave as a large accelerator with respect to the host CPU. Loosely-coupled accelerators for graph applications have been investigated before, e.g. [19]. However, ASIC accelerators cannot execute the variety of workloads that software-programmable processors can. Dalorex is not

restricted to executing graph applications and can be used for other domains since it is software programmable.

Unlike the prior work, which assumes an HMC technology that has not been adopted, there is already an example of an architecture where all the memory is distributed on-chip being commercialized by Cerebras [9], [35] to speed up Machine Learning applications. As we show in this study, the Dalorex execution model, and design decisions like network type, local memory size, and task scheduling, can unleash an outstanding graph processing performance for distributed memory architectures.

Another example of an architecture that could use Dalorex is a regular memory hierarchy with large L1 caches per tile, leveraging prior work in cache-scratchpad duality [11], [13], [30] to provide a hybrid solution that would benefit both cache-averse and cache-friendly workloads.

VII. CONCLUSION

We found that reaching the parallelization limits of graph processing requires: (1) a *uniform work balance*, which we achieve with an equal amount of data per tile; (2) architectural and programming *support to invoke remote tasks natively* with no message overhead; (3) a *traffic-aware* arbitration of tasks; (4) a *NoC that minimizes contention*, where a torus is superior to the mesh; and (5) a *NoC that scales bisection bandwidth* with very large tile counts on a 2D silicon, where we found *ruce channels* compelling.

In addition, since each tile owns a chunk of the vertex array, we found that we could support a barrierless frontier without extra cost. Although the work balance is optimal if the hot vertices of the graph are uniformly distributed, we found that removing the global frontier further helped avoid processors waiting for the slowest one at the end of each epoch.

Combined, these optimizations made Dalorex two orders of magnitude faster and more energy-efficient than the state-of-the-art in accelerating graph processing.

REFERENCES

- [1] M. Abeydeera and D. Sanchez, “Chronos: Efficient speculative parallelism for accelerators,” in *Proceedings of the Twenty-Fifth International Conference on Architectural Support for Programming Languages and Operating Systems*, 2020, pp. 1247–1262.
- [2] J. Ahn, S. Hong, S. Yoo, O. Mutlu, and K. Choi, “A scalable processing-in-memory accelerator for parallel graph processing,” in *Proceedings of the 42nd Annual International Symposium on Computer Architecture*, 2015, pp. 105–117.
- [3] “Apache Giraph,” The Apache Software Foundation, <http://giraph.apache.org/>.
- [4] J. Balkind, M. McKeown, Y. Fu, T. Nguyen, Y. Zhou, A. Lavrov, M. Shahradd, A. Fuchs, S. Payne, X. Liang, M. Matl, and D. Wentzlaff, “OpenPiton: An open source manycore research framework,” in *ASPLOS*. ACM, 2016, pp. 217–232.
- [5] S. Beamer, K. Asanovic, and D. Patterson, “Direction-optimizing breadth-first search,” in *SC ’12: Proceedings of the International Conference on High Performance Computing, Networking, Storage and Analysis*, 2012, pp. 1–10.
- [6] S. Beamer, K. Asanovic, and D. Patterson, “The gap benchmark suite,” *arXiv preprint arXiv:1508.03619*, 2015.
- [7] M. Besta, M. Podstawski, L. Groner, E. Solomonik, and T. Hoefler, “To push or to pull: On reducing communication and synchronization in graph computations,” *CoRR*, vol. abs/2010.16012, 2020. [Online]. Available: <https://arxiv.org/abs/2010.16012>

- [8] E. G. Boman, K. D. Devine, and S. Rajamanickam, "Scalable matrix computations on large scale-free graphs using 2d graph partitioning," in *Proceedings of the International Conference on High Performance Computing, Networking, Storage and Analysis*, 2013, pp. 1–12.
- [9] Cerebras Systems Inc., "The second generation wafer scale engine," <https://cerebras.net/wp-content/uploads/2021/04/Cerebras-CS-2-Whitepaper.pdf>.
- [10] T.-Y. J. Chang, Y.-H. Chen, W.-M. Chan, H. Cheng, P.-S. Wang, Y. Lin, H. Fujiwara, R. Lee, H.-J. Liao, P.-W. Wang, G. Yeap, and Q. Li, "A 5-nm 135-mb sram in euv and high-mobility channel finfet technology with metal coupling and charge-sharing write-assist circuitry schemes for high-density and low- α applications," *IEEE Journal of Solid-State Circuits*, vol. 56, no. 1, pp. 179–187, 2021.
- [11] C. C. Chou, A. Jaleel, and M. K. Qureshi, "Cameo: A two-level memory organization with capacity of main memory and flexibility of hardware-managed cache," in *2014 47th Annual IEEE/ACM International Symposium on Microarchitecture*. IEEE, 2014, pp. 1–12.
- [12] E. Cota, G. D. Guglielmo, P. Mantovani, and L. Carloni, "An analysis of accelerator coupling in heterogeneous architectures," in *Proceedings of the 52nd Design Automation Conference (DAC)*, 2015.
- [13] E. G. Cota, P. Mantovani, and L. P. Carloni, "Exploiting private local memories to reduce the opportunity cost of accelerator integration," in *Proceedings of the 2016 International Conference on Supercomputing*, 2016, pp. 1–12.
- [14] V. Dadu, S. Liu, and T. Nowatzki, "Polygraph: Exposing the value of flexibility for graph processing accelerators," in *2021 ACM/IEEE 48th Annual International Symposium on Computer Architecture (ISCA)*. IEEE, 2021, pp. 595–608.
- [15] S. Davidson, S. Xie, C. Torng, K. Al-Hawai, A. Rovinski, T. Ajayi, L. Vega, C. Zhao, R. Zhao, S. Dai, A. Amarnath, B. Veluri, P. Gao, A. Rao, G. Liu, R. K. Gupta, Z. Zhang, R. Dreslinski, C. Batten, and M. B. Taylor, "The celerity open-source 511-core risc-v tiered accelerator fabric: Fast architectures and design methodologies for fast chips," *IEEE Micro*, vol. 38, no. 2, pp. 30–41, 2018.
- [16] S. Enjapuri, D. Gujjar, S. Sinha, R. Halli, and M. Trivedi, "A 5nm wide voltage range ultra high density sram design for l2/l3 cache applications," in *2021 34th International Conference on VLSI Design and 2021 20th International Conference on Embedded Systems (VLSID)*, 2021, pp. 151–156.
- [17] Esperanto Technologies, "Esperanto's et-minion on-chip risc-v cores," <https://www.esperanto.ai/technology/>.
- [18] T. J. Ham, J. L. Aragón, and M. Martonosi, "DeSC: Decoupled supply-compute communication management for heterogeneous architectures," in *MICRO*. ACM, 2015.
- [19] T. J. Ham, L. Wu, N. Sundaram, N. Satish, and M. Martonosi, "Graphicionado: A high-performance and energy-efficient accelerator for graph analytics," in *Proceedings of the 49th Annual International Symposium on Microarchitecture*, ser. MICRO, 2016. [Online]. Available: <https://doi.org/10.1109/MICRO.2016.7783759>
- [20] M. Han and K. Daudjee, "Giraph unchained: Barrierless asynchronous parallel execution in pregel-like graph processing systems," *Proceedings of the VLDB Endowment*, vol. 8, no. 9, pp. 950–961, 2015.
- [21] J. L. Hennessy and D. A. Patterson, "A new golden age for computer architecture," *Communications of the ACM*, vol. 62, no. 2, pp. 48–60, 2019.
- [22] R. Ho, K. W. Mai, and M. A. Horowitz, "The future of wires," *Proceedings of the IEEE*, vol. 89, no. 4, pp. 490–504, 2001.
- [23] H. Hoffmann, "Stream algorithms and architecture," Ph.D. dissertation, Massachusetts Institute of Technology, 2003.
- [24] "Hybrid Memory Cube (HMC)," <http://www.hybridmemorycube.org>, 2018.
- [25] K. T. Johnson, A. R. Hurson, and B. Shirazi, "General-purpose systolic arrays," *Computer*, vol. 26, no. 11, pp. 20–31, 1993.
- [26] N. P. Jouppi, C. Young, N. Patil, D. Patterson, G. Agrawal, R. Bajwa, S. Bates, S. Bhatia, N. Boden, A. Borchers *et al.*, "In-datacenter performance analysis of a tensor processing unit," in *Proceedings of the 44th annual international symposium on computer architecture*, 2017, pp. 1–12.
- [27] D. C. Jung, S. Davidson, C. Zhao, D. Richmond, and M. B. Taylor, "Ruche networks: Wire-maximal, no-fuss nocs: Special session paper," in *2020 14th IEEE/ACM International Symposium on Networks-on-Chip (NOCS)*. IEEE, 2020, pp. 1–8.
- [28] G. Karypis and V. Kumar, "Metis: A software package for partitioning unstructured graphs," *Partitioning Meshes, and Computing Fill-Reducing Orderings of Sparse Matrices, Version*, vol. 4, no. 0, 1998.
- [29] S. Knowles, "Graphcore," in *2021 IEEE Hot Chips 33 Symposium (HCS)*. IEEE, 2021, pp. 1–25.
- [30] S. Kumar, H. Zhao, A. Shiraman, E. Matthews, S. Dwarkadas, and L. Shannon, "Amoeba-cache: Adaptive blocks for eliminating waste in the memory hierarchy," in *2012 45th Annual IEEE/ACM International Symposium on Microarchitecture*. IEEE, 2012, pp. 376–388.
- [31] T. S. Kumar and S. L. Tripathi, "Process evaluation in finfet based 7t sram cell," *Analog Integrated Circuits and Signal Processing*, pp. 1–7, 2021.
- [32] H. T. Kung and C. E. Leiserson, "Systolic arrays for (vlsi)." Carnegie-Mellon University, Tech. Rep., 1978.
- [33] P. Lawrence, B. Sergey, R. Motwani, and T. Winograd, "The pagerank citation ranking: Bringing order to the web," Stanford University, Technical Report, 1998.
- [34] J. Leskovec, D. Chakrabarti, J. Kleinberg, C. Faloutsos, and Z. Ghahramani, "Kronecker graphs: An approach to modeling networks," *Journal of Machine Learning Research (JMLR)*, vol. 11, pp. 985–1042, Mar. 2010.
- [35] S. Lie, "Multi-million core, multi-wafer ai cluster," in *2021 IEEE Hot Chips 33 Symposium (HCS)*. IEEE Computer Society, 2021, pp. 1–41.
- [36] G. Malewicz, M. H. Austern, A. J. Bik, J. C. Dehnert, I. Horn, N. Leiser, and G. Czajkowski, "Pregel: a system for large-scale graph processing," in *Proceedings of the 2010 ACM SIGMOD International Conference on Management of data*, 2010, pp. 135–146.
- [37] A. Manocha, T. Sorensen, E. Tureci, O. Matthews, J. L. Aragón, and M. Martonosi, "Graphattack: Optimizing data supply for graph applications on in-order multicore architectures," *ACM Transactions on Architecture and Code Optimization (TACO)*, vol. 18, no. 4, pp. 1–26, 2021.
- [38] M. McKeown, A. Lavrov, M. Shahrad, P. J. Jackson, Y. Fu, J. Balkind, T. M. Nguyen, K. Lim, Y. Zhou, and D. Wentzlaff, "Power and energy characterization of an open source 25-core manycore processor," in *HPCA*, 2018, pp. 762–775.
- [39] G. E. Moore, "Cramming more components onto integrated circuits," *Proceedings of the IEEE*, vol. 86, no. 1, pp. 82–85, 1998.
- [40] A. Mukkara, N. Beckmann, and D. Sanchez, "PHI: Architectural Support for Synchronization-and Bandwidth-Efficient Commutative Scatter Updates," in *Proceedings of the 52nd annual IEEE/ACM international symposium on Microarchitecture (MICRO-52)*, October 2019.
- [41] Q. M. Nguyen and D. Sanchez, "Pipette: Improving core utilization on irregular applications through intra-core pipeline parallelism," in *2020 53rd Annual IEEE/ACM International Symposium on Microarchitecture (MICRO)*. IEEE, 2020, pp. 596–608.
- [42] Q. M. Nguyen and D. Sanchez, "Fifer: Practical acceleration of irregular applications on reconfigurable architectures," in *MICRO-54: 54th Annual IEEE/ACM International Symposium on Microarchitecture*, ser. MICRO '21. New York, NY, USA: Association for Computing Machinery, 2021, p. 1064–1077. [Online]. Available: <https://doi.org/10.1145/3466752.3480048>
- [43] T. M. Nguyen and D. Wentzlaff, "Morc: A manycore-oriented compressed cache," in *Proceedings of the 48th International Symposium on Microarchitecture*, 2015, pp. 76–88.
- [44] M. Orenes-Vera, A. Manocha, J. Balkind, F. Gao, J. L. Aragón, D. Wentzlaff, and M. Martonosi, "Tiny but mighty: designing and realizing scalable latency tolerance for manycore socs," in *ISCA*, 2022, pp. 817–830.
- [45] Y. Ou, S. Agwa, and C. Batten, "Implementing low-diameter on-chip networks for manycore processors using a tiled physical design methodology," in *2020 14th IEEE/ACM International Symposium on Networks-on-Chip (NOCS)*. IEEE, 2020, pp. 1–8.
- [46] M. M. Ozdal, S. Yesil, T. Kim, A. Ayupov, J. Greth, S. Burns, and O. Ozturk, "Energy efficient architecture for graph analytics accelerators," *ACM SIGARCH Computer Architecture News*, vol. 44, no. 3, pp. 166–177, 2016.
- [47] J. T. Pawlowski, "Hybrid memory cube (hmc)," in *2011 IEEE Hot Chips 23 Symposium (HCS)*. IEEE, 2011, pp. 1–24.
- [48] L. Piccolboni, P. Mantovani, G. Di Guglielmo, and L. P. Carloni, "Broadening the exploration of the accelerator design space in embedded scalable platforms," in *HPEC*. IEEE Press, 2017.
- [49] S. H. Pugsley, J. Jestes, H. Zhang, R. Balasubramanian, V. Srinivasan, A. Buyuktosunoglu, A. Davis, and F. Li, "Ndc: Analyzing the impact of

- 3d-stacked memory+ logic devices on mapreduce workloads,” in *2014 IEEE International Symposium on Performance Analysis of Systems and Software (ISPASS)*. IEEE, 2014, pp. 190–200.
- [50] S. Rahman, N. Abu-Ghazaleh, and R. Gupta, “Graphpulse: An event-driven hardware accelerator for asynchronous graph processing,” in *2020 53rd Annual IEEE/ACM International Symposium on Microarchitecture (MICRO)*. IEEE, 2020, pp. 908–921.
- [51] K. Rupp, “42 Years of Microprocessor Trend Data,” <https://www.karlsruhp.net/2018/02/42-years-of-microprocessor-trend-data/>, 2018.
- [52] D. Sanchez and C. Kozyrakis, “Zsim: Fast and accurate microarchitectural simulation of thousand-core systems,” *ACM SIGARCH Computer architecture news*, vol. 41, no. 3, pp. 475–486, 2013.
- [53] G. M. Slota, S. Rajamanickam, and K. Madduri, “BFS and coloring-based parallel algorithms for strongly connected components and related problems,” in *2014 IEEE 28th International Parallel and Distributed Processing Symposium, Phoenix, AZ, USA, May 19-23, 2014*. IEEE Computer Society, 2014, pp. 550–559. [Online]. Available: <https://doi.org/10.1109/IPDPS.2014.64>
- [54] A. Stillmaker and B. Baas, “Scaling equations for the accurate prediction of cmos device performance from 180 nm to 7 nm,” *Integration*, vol. 58, pp. 74–81, 2017.
- [55] N. Talati, K. May, A. Behroozi, Y. Yang, K. Kaszyk, C. Vasiladiotis, T. Verma, L. Li, B. Nguyen, J. Sun, J. M. Morton, A. Ahmadi, T. Austin, M. O’Boyle, S. Mahlke, T. Mudge, and R. Dreslinski, “Prodigy: Improving the memory latency of data-indirect irregular workloads using hardware-software co-design,” in *2021 IEEE International Symposium on High-Performance Computer Architecture (HPCA)*. IEEE, 2021, pp. 654–667.
- [56] M. Taylor, W. Lee, S. P. Amarasinghe, and A. Agarwal, “Scalar operand networks,” *IEEE Transactions on Parallel and Distributed Systems*, vol. 16, no. 2, pp. 145–162, 2005.
- [57] M. B. Taylor, J. Kim, J. Miller, D. Wentzlaff, F. Ghodrat, B. Greenwald, H. Hoffman, P. Johnson, J.-W. Lee, W. Lee *et al.*, “The raw microprocessor: A computational fabric for software circuits and general-purpose programs,” *IEEE micro*, vol. 22, no. 2, pp. 25–35, 2002.
- [58] M. Technology, “Ddr3/ddr4 system-power calculator,” <https://www.micron.com/support/tools-and-utilities/power-calc>.
- [59] Y. Tian, A. Balmin, S. A. Corsten, S. Tatikonda, and J. McPherson, “From” think like a vertex” to” think like a graph”,” *Proceedings of the VLDB Endowment*, vol. 7, no. 3, pp. 193–204, 2013.
- [60] Q. Xie, X. Lin, Y. Wang, S. Chen, M. J. Dousti, and M. Pedram, “Performance comparisons between 7-nm finfet and conventional bulk cmos standard cell libraries,” *IEEE Transactions on Circuits and Systems II: Express Briefs*, vol. 62, no. 8, pp. 761–765, 2015.
- [61] Y. Yokoyama, M. Tanaka, K. Tanaka, M. Morimoto, M. Yabuuchi, Y. Ishii, and S. Tanaka, “A 29.2 mb/mm² ultra high density sram macro using 7nm finfet technology with dual-edge driven wordline/bitline and write/read-assist circuit,” in *2020 IEEE Symposium on VLSI Circuits*, 2020, pp. 1–2.
- [62] H. Yoshida, Y. Shiotsu, D. Kitagata, S. Yamamoto, and S. Sugahara, “Ultralow-voltage retention sram with a power gating cell architecture using header and footer power-switches,” *IEEE Open Journal of Circuits and Systems*, vol. 2, pp. 520–533, 2021.
- [63] F. Zaruba and L. Benini, “The cost of application-class processing: Energy and performance analysis of a linux-ready 1.7-ghz 64-bit risc-v core in 22-nm fdsoi technology,” *IEEE Transactions on Very Large Scale Integration (VLSI) Systems*, vol. 27, no. 11, pp. 2629–2640, Nov 2019, <https://github.com/openhwgroup/cva6>.
- [64] F. Zaruba and L. Benini, “Ariane: An open-source 64-bit RISC-V application class processor and latest improvements,” 2018, technical talk at the RISC-V Workshop <https://www.youtube.com/watch?v=8HpVRNh0ux4>.
- [65] F. Zaruba, F. Schuiki, and L. Benini, “Manticore: A 4096-core risc-v chiplet architecture for ultraefficient floating-point computing,” *IEEE Micro*, vol. 41, no. 2, pp. 36–42, 2020.
- [66] F. Zaruba, F. Schuiki, T. Hoeffler, and L. Benini, “Snitch: A tiny pseudo dual-issue processor for area and energy efficient execution of floating-point intensive workloads,” *IEEE Transactions on Computers*, 2020.
- [67] M. Zhang, Y. Zhuo, C. Wang, M. Gao, Y. Wu, K. Chen, C. Kozyrakis, and X. Qian, “Graphp: Reducing communication for pim-based graph processing with efficient data partition,” in *2018 IEEE International Symposium on High Performance Computer Architecture (HPCA)*. IEEE, 2018, pp. 544–557.
- [68] Y. Zhang, M. Yang, R. Baghdadi, S. Kamil, J. Shun, and S. Amarasinghe, “Graphit: A high-performance graph dsl,” *Proceedings of the ACM on Programming Languages*, vol. 2, no. OOPSLA, pp. 1–30, 2018.
- [69] P. Zhou, J. Hom, G. Upadhyaya, K. Goodson, and M. Munch, “Electrokinetic microchannel cooling system for desktop computers,” in *Twentieth Annual IEEE Semiconductor Thermal Measurement and Management Symposium (IEEE Cat. No. 04CH37545)*. IEEE, 2004, pp. 26–29.
- [70] X. Zhu, W. Chen, W. Zheng, and X. Ma, “Gemini: A computation-centric distributed graph processing system,” in *12th {USENIX} symposium on operating systems design and implementation ({OSDI} 16)*, 2016, pp. 301–316.
- [71] Y. Zhu, B. Wang, D. Li, and J. Zhao, “Integrated thermal analysis for processing in die-stacking memory,” in *Proceedings of the Second International Symposium on Memory Systems*, 2016, pp. 402–414.
- [72] Y. Zhuo, C. Wang, M. Zhang, R. Wang, D. Niu, Y. Wang, and X. Qian, “Graphq: Scalable pim-based graph processing,” in *Proceedings of the 52nd Annual IEEE/ACM International Symposium on Microarchitecture*, 2019, pp. 712–725.